European Cells and Materials Vol.47 2024 (pages 253–264) DOI: 10.22203/eCM.v047a16 ISSN 1473-2262

Original Article

MATRIX STIFFNESS REGULATES BMSCs OSTEOGENIC DIFFERENTIATION THROUGH AN AUTOPHAGY-DEPENDENT MANNER

B.Q. Wang[1,2,3,4], Y.Q. Yang[1,3], H.F. Xie[2,3,4,*] and C.Y. Xue[1,3,4,*]

[1]Department of Oral Implantology, The Affiliated Stomatological Hospital of Nanjing Medical University, 210029 Nanjing, Jiangsu, China
[2]Department of Prosthodontics, The Affiliated Stomatological Hospital of Nanjing Medical University, 210029 Nanjing, Jiangsu, China
[3]State Key Laboratory Cultivation Base of Research, Prevention and Treatment for Oral Diseases, Nanjing Medical University, 210029 Nanjing, Jiangsu, China
[4]Jiangsu Province Engineering Research Center of Stomatological Translational Medicine, Nanjing Medical University, 210029 Nanjing, Jiangsu, China

Abstract

In the field of bone tissue engineering, scaffold materials play a central role in restoring and regenerating the physiological function of the skeletal system. Mechanical signals in the cellular microenvironment significantly influence cellular behavior, and the selection of an appropriate scaffold matrix is crucial in guiding precursor cells towards their desired cell fate. The aim of this study is to investigate the impact of matrix stiffness on osteogenic differentiation of bone marrow mesenchymal stem cells (BMSCs) and whether matrix stiffness affects BMSCs osteogenic differentiation in an autophagy-dependent manner. BMSCs were co-cultured with transglutaminase (TG)-Gelatin (Gel) matrices of varying stiffness, and subsequently, osteogenic markers in each experimental group were evaluated. Additionally, the levels of autophagy within the cells were quantitatively measured. Furthermore, inhibitor experiments were conducted to gain deeper insights into potential mechanisms. We observed that within a certain range of stiffness, autophagy levels increased with the augmentation of matrix stiffness, leading to an elevation in the levels of osteogenesis-related molecules.

Keywords: Bone marrow mesenchymal stem cells, matrix stiffness, extracellular matrix, osteogenic differentiation, autophagy.

***Address for correspondence**: H.F. Xie, Department of Prosthodontics, The Affiliated Stomatological Hospital of Nanjing Medical University, 210029 Nanjing, Jiangsu, China; State Key Laboratory Cultivation Base of Research, Prevention and Treatment for Oral Diseases, Nanjing Medical University, 210029 Nanjing, Jiangsu, China; Jiangsu Province Engineering Research Center of Stomatological Translational Medicine, Nanjing Medical University, 210029 Nanjing, Jiangsu, China. Email: xhf-1980@126.com; C.Y. Xue, Department of Oral Implantology, The Affiliated Stomatological Hospital of Nanjing Medical University, 210029 Nanjing, Jiangsu, China; State Key Laboratory Cultivation Base of Research, Prevention and Treatment for Oral Diseases, Nanjing Medical University, 210029 Nanjing, Jiangsu, China; Jiangsu Province Engineering Research Center of Stomatological Translational Medicine, Nanjing Medical University, 210029 Nanjing, Jiangsu, China. Email: xuechangyue@njmu.edu.cn

Introduction

Bone defects is a common complication in trauma, tumor removal, congenital issues, infections, or reconstructive surgical procedures. The restoration of normal physiological function in bones is essential for treating human diseases and repairing defects. Tissue engineering scaffolds aim to create an active microenvironment conducive to bone formation, promoting local tissue and cell regeneration. The extracellular matrix (ECM) is a critical component of this microenvironment, providing structural support and regulating cellular behavior during vascular and skeletal development (Shao *et al*., 2022; Zeng *et al*., 2023). Hydrogels, as a type of biomaterials, provide a suitable microenvironment for bone tissue and osteochondral engineering to control cell morphology, proliferation, and differentiation. For instance, the 3D bioprinting osteochondral constructs of MSC-laden GelMA-based hydrogel achieved high cell density and viability to promote cell adhesion, osteogenic differentiation, and bone matrix deposition by MSCs (Levato *et al*., 2014). Mechanical stimuli within the microenvironment, especially matrix stiffness, significantly impact cell behavior. For example, Studies have revealed that increased stiffness led to osteogenic differentiation, while decreased stiffness resulted in chondrogenic differentiation in mesenchymal cells (MSCs) (Steinmetz *et al*., 2015). Although the effects of matrix stiffness in the

regulation of osteogenic differentiation have been investigated, the mechanism by which matrix stiffness affects osteogenic differentiation of bone marrow mesenchymal stem cells (BMSCs) remains unclear.

Physiologically, bones undergo continuous reabsorption, formation, and remodeling. Autophagy is an essential metabolic process in eukaryotic cells and plays a vital role in bone regeneration. Since mechanical stimulation has the capability to trigger autophagy through specialized sensors. Autophagy maintains cellular balance by disassembling and eliminating damaged proteins and organelles to play a notable part in preosteoblast differentiation, the transformation from osteoblasts to osteocytes, and the development and operation of osteoclasts (Husain and Jeffries, 2017; Shapiro *et al*., 2014; Smith and Wilkinson, 2017). Mechanistic study shows that autophagy regulates osteoblast mineralization, osteoclast differentiation and chondrocyte differentiation. In osteoblasts, autophagy deficiency in osteoblasts decreases their mineralizing capacity and triggers an imbalance between osteoblasts and osteoclasts resulting in a low bone mass phenotype (Nollet *et al*., 2014). In osteoclasts, proteins essential for autophagy, including Atg5, Atg7, Atg4B, and LC3, are important for generating the osteoclast ruffled border, the secretory function of osteoclasts, and bone resorption *in vitro* and *in vivo* (DeSelm *et al*., 2011). Whether matrix stiffness affects BMSCs osteogenic differentiation in an autophagy-dependent manner is still unknown.

In this study, we developed a transglutaminase (TG)-Gel (Gelatin) model with adjustable matrix stiffness. The impact of substrate stiffness on BMSC osteogenesis was observed through osteogenesis staining and detection of osteogenic markers. And the autophagy level of cells in matrix of various stiffness were determined through Monodansylcadaverine (MDC) staining and detection of autophagy markers. The current hypothesis of this study is that, within a certain stiffness range in TG-Gel, autophagy increased along with the increase of substrate stiffness, which leads to increased levels of osteogenesis-related molecules.

Materials and Methods

Cell Culture and Identification

This study adhered to ethical principles and received approval from the Experimental Animal Welfare Ethics Committee of Nanjing Medical University (IACUC-2203005) for the protocols employed. BMSCs were acquired from 12-week-old male SD rats sourced from the Animal Core Facility of Nanjing Medical University. After cervical dislocation under anaesthesia (2 % pentobarbital sodium, 0.3 mL/100 g ip), the jaw bone of SD rats was flushed with PBS, and the mandible was cut into 5 mm bone pieces. Cells were initially seeded at a concentration of 1×10^6 cells/mL in α-medium (Gibco, Grand Island, NY, USA) supplemented with 10 % FBS (Gibco) and 1 % penicillin/streptomycin (Gibco). All cells were kept in incubator (Thermo Scientific, Waltham, MA, USA) at 37 °C with 5 % CO_2. To characterize BMSCs, flow cytometry was employed to analyze the expression levels of CD34, CD45, CD73, and CD90. In brief, cells were trypsinized to create cell suspensions at a concentration of 2×10^7/mL. Subsequently, these suspensions were incubated with labeled antibodies, including CD73 (Clone QA20A48, BioLegend, San Diego, CA, USA), CD34 (Clone HM34, BioLegend), CD45 (Clone S18009F, BioLegend), and CD90 (Clone 5E10, BioLegend), for a duration of 45 minutes. Isotype controls were used for each antibody. Finally, the results were analyzed using BD FACSAriaII (BD Biosciences, San Jose, CA, USA).

To trigger adipogenic differentiation, BMSCs were exposed to an adipogenic-inducing medium (RAXMX-90031, OriCell, Guangzhou, China) for a duration of 21 days. The confirmation of adipogenic induction was achieved through oil red O staining.

Fabrication of TG-Gel of Varying Stiffnesses

Gelatin (9000-70-8, Aladdin, Shanghai, China) was dissolved in distilled water and then autoclaved to create an 18 % gelatin stock. The sterilized gelatin was divided into portions and kept at 4 °C until needed. To modulate the stiffness of the hydrogel-based ECM, the 18 % gelatin was initially liquefied by heating it in a water bath at a temperature of 60 °C. Gelatin solutions of varying concentrations (2 %, 4 %, 6 %, and 8 %) were prepared by diluting an 18 % gelatin stock in PBS. The higher the gelatin concentration, the greater the matrix stiffness. Transglutaminase (TG) from *Streptomyces mobaraensis* was kindly supplied by Macklin, Shanghai. TG achieved the covalent binding of the gel's by ε-amino group of lysine and the γ-carboxamide group of glutamine. It's possible that the initial measurements of stiffness and porosity of the TG-Gel might not accurately reflect the final values observed towards the end of the study. This discrepancy could arise from the potential degradation of TG-Gel caused by the enzymatic activities of collagenase and MMPs over time.

The TG-Gel was formulated by stepwise blending sterile ingredients (Table 1) such as (a) 2 %, 4 %, 6 %, and 8 % gelatin; (b) rat tail tendon collagen type I; (c) the cell suspension and medium was added; (d) and the TG was added to a tube and thoroughly mixed; (e) the mixture was inoculated in 48-well plates and placed in the incubator (Fig. 1**c**).

The Young's modulus of various hydrogels was assessed using a Universal Testing System (R3365, Instron, Norwood, MA, USA), and the hydrogel stiffness was computed employing the subsequent formula:

$$K = EA/L$$

In this equation, K represents stiffness, E denotes Young's modulus, A signifies the cross-sectional area, and L stands for the height of the hydrogel.

Table 1. Reagent volumes for the setup of hydrogels at different stiffness.

Regent \ Proportion	2 %	4 %	6 %	8 %
PBS (µL)	44.5	39.0	33.0	28.0
18 % Gelatin (µL)	5.5	11.0	17.0	22.0
Rat tail tendon collagen type I (µL)	1.0	1.0	1.0	1.0
Cell Suspension (µL)	25.0	25.0	25.0	25.0
TG (µL)	10.0	10.0	10.0	10.0
Total (µL)	86.0	86.0	86.0	86.0

TG, Transglutaminase.

Encapsulation of BMSCs within TG-Gel for 3D Cultivation

For BMSCs encapsulation, the gelatin was initially liquefied by heating it in a water bath at a temperature of 60 °C. Then each 50 µL of the gelatin solution (2 %, 4 %, 6 % or 8 %) was mixed with BMSCs at a density of 2 × 10^6 cells/mL. 10 µL of transglutaminase were added to crosslink the gelatin, and 1 µL of the rat tail tendon collagen type I was added to promote cell adhesion. TG-Gel mixture were seeded into a 48-well culture plate. When the TG-gels had solidified through chemical cross-linking, 500 µL of osteogenic induction medium was added to each well.

Porosity Measurement

The porosity of the produced TG-Gel was determined using the liquid displacement technique (Guan *et al*., 2005; Zhang and Ma, 1999). In short, the TG-Gel was submerged in a graduated cylinder containing a predetermined volume (V_1) of ethanol for a duration of 5 minutes. Ethanol served as the displacing solution due to its effective penetration into the pores without causing any shrinkage or swelling, as it is a non-solvent for the TG-Gel. The combined volume of ethanol with the ethanol-soaked hydrogel was noted as V_2. Subsequently, the ethanol-saturated hydrogel was extracted from the cylinder, and the remaining ethanol volume was recorded as V_3. The porosity of the TG-Gel was quantified using the formula $p = (V_1 - V_3)/(V_2 - V_3) \times 100$ %.

Cytotoxicity Assays

Each hydrogel sample had a surface area of 2.09 cm^2 (approximately 86 µL each). To prepare a hydrogel extract solution, TG-Gel were then transferred to centrifuge tubes, followed by the addition of α-MEM. All TG-Gel with varied stiffness samples were subsequently incubated for 72 hours at 37 °C in darkness. The ratio of the sample's surface area to the solution volume was roughly 2.39 cm^2/mL, which falls within the suggested range of 0.5–6.0 cm^2/mL as specified by ISO standards (ISO S. Biological evaluations of medical devices. Part 12. Sample preparation and reference materials 1996; 12).

BMSCs' viability was assessed using the Cell Counting Kit-8 (CCK-8) as they were exposed to respective extract solutions corresponding to each group within 96-well plates. The cell density was 1 × 10^5 cells/mL. BMSCs were cultured in respective extract solutions corresponding to each group of interest. During this procedure, eluates were introduced, and the plates were incubated for 2 hours. Control cells were solely provided with the medium. Following two washes with PBS, cells were placed in 110 µL of working solution (a mixture of CCK-8 stock solution and α-medium at a 1:10 ratio) for 2 hours. Afterward, the absorbance was recorded using a multiplate reader at 450 nm (Molecular Devices, San Jose, CA, USA).

Transmission Electron Microscopy Analysis

BMSCs were cultured on the surface of hydrogels of two groups for 7 days, followed by fixation using 3 % glutaraldehyde. The control group was treated with regular complete culture medium, while the other group was treated with osteogenic induction medium. Samples were subsequently post-fixed in a 1 % osmium tetroxide solution for 1 hour. The cells were then embedded in a gold-palladium solution. Ultrathin sections were examined using a transmission electron microscope (HT7800, Hitachi, Tokyo, Japan). For each specimen, at least 10^6 cells were assessed by an observer who was unaware of the experimental conditions to determine the quantity of autophagosomes per cell.

Osteogenesis Staining Analysis

Alkaline phosphatase (ALP) serves as an early indicator of osteogenic differentiation and functional maturation. After BMSCs encapsulated within TG-Gel, each group (2 %, 4 %, 6 %, 8 %) was cultured in osteogenic induction medium (α-MEM, 10 % FBS, 50 µg/mL VC, 100 nM dexamethasone, 10 mM β-glycerophosphate, 1 % penicillin/streptomycin) at 37 °C with 5 % CO_2 for 7 days. TG-Gel were washed twice with PBS, then incubated with 500 µL of 0.25 % trypsin for 3 hours to release the cells from the hydrogel. Subsequently, the cells were fixed with 4 % paraformaldehyde (BL539A, Biosharp, Guangzhou, China) for 30 minutes, followed by staining according to the instructions of the BCIP/NBT alkaline phosphatase chromogenic kit (P0321S, Beyotime, Shanghai, China), and images were captured to analyze early osteogenic differentiation. For quantitative detection of ALP activity in BMSCs, procedures outlined in the ALP activity assay kit (P0321, Beyotime) were followed. Absorbance was measured using a microplate spectrophotometer. Additionally, Pearson correlation analysis was performed using SPSS software (version 26.0; IBM, NY, USA) to assess the correlation between matrix stiffness and ALP levels. Matrix stiffness values and ALP levels were treated as two variables for analysis, and the correlation coefficient was calculated.

To assess the extent of calcium deposition as a late marker of bone formation, Alizarin Red S staining was conducted after osteogenic induction 21 days. The TG-Gel

construct underwent two PBS washes, followed by fixation in 4 % paraformaldehyde for 30 minutes. Subsequently, it was stained with Alizarin Red S (40 mM, pH 4.2) (C0148S, Beyotime) for 30 minutes. After staining, the sample underwent two rinses with ddH_2O to eliminate any non-specific precipitates. The presence of positive orange-red staining signified calcium deposition by the BMSCs. Images were taken to analyze late-stage osteogenic differentiation.

Monodansylcadaverine (MDC) Staining

MDC can specifically label autophagosomes. Following rinsing with Earle's balanced salt solution (EBSS) (C0213, Beyotime), BMSCs within the hydrogel were subjected to EBSS treatment at 37 °C for 40 min in an incubator. Next, the cells underwent three PBS washes. Then, the construct was treated with an Autophagy Staining Assay Kit with MDC (C3018S, Beyotime) at 37 °C for 30 min at darkness. The visualization of MDC-stained vacuoles was determined by inverted microscopy (DMI3000B, Leica, Wetzlar, Germany). Optical density, cell counts, and cell areas were evaluated through ImageJ software (version 1.52; NIH, Bethesda, MD, USA). The optical density was computed using the formula: average optical density = MDC fluorescence intensity per cell/cell area.

Immunofluorescence

Following a 7-day incubation period, BMSCs on different TG-Gel substrates were initially fixed using 4 % paraformaldehyde and subsequently made permeable with 0.5 % Triton X-100 (P0096, Beyotime). Following permeabilization, samples were blocked using 5 % sheep serum (AR009, Boster, Wuhan, China), and immunofluorescence was conducted using primary antibodies against Runx2 (Abcam, Cambridge, UK) and ATG5 (YM3752, Immu Noway, Newark, CA, USA). Goat anti-rabbit coralite594 conjugate (1:200) (SA00013-4, Proteintech, Chicago, IL, USA) and goat anti-mouse coralite488 conjugate (1:200) (SA00013-1, Proteintech) were used as secondary antibodies. DAPI (F6057, Sigma–Aldrich, St. Louis, MO, USA) was used to stain nuclei. To observe the morphologies of BMSCs, images were captured by a positive fluorescence microscope (DM4000, Leica).

Extraction of RNA and Analysis of Gene Expression

The total RNA from BMSCs cultured in the hydrogel was extracted employing an animal RNA isolation kit with a spin column (R0026, Beyotime). The reverse transcription reaction was performed with a synthesis kit (R233-01, Vazyme, Nanjing, China) according to the manufacturer's instructions. RT-PCR was conducted using one-step SYBR Green reagents, following the manufacturer's instructions (11202ES03, Yeasen, Shanghai, China), and employing the ABI Q7 PCR machine (Applied Biosystems, Foster City, CA, USA). Target gene expression was normalized with reference to the GAPDH gene through the $2^{-\Delta\Delta Ct}$ method. The primers for amplification, obtained from Sangon Biotech, China, are detailed in Table 2.

Western Blot Analysis

To detach the cells from the TG-Gel, 500 µL of 0.25 % trypsin per well was added, and the mixture was incubated for 8 hours. Protein samples were combined with SDS–PAGE Sample Loading Buffer (P0015A, Beyotime) and then boiled at 100 °C for 5 minutes. Proteins were separated using SDS-polyacrylamide gels. The proteins were then incubated overnight with antibodies specific to GAPDH, BMP2, osteocalcin (OCN), RUNX2, LC3, Beclin-1, and ATG5. Subsequently, the membranes were exposed to secondary antibodies (Abbkine, Wuhan, China). Signal detection was carried out using the Tanon5200 system (Tannon,Shanghai,China), and quantification was performed using ImageJ software.

Inhibitor Experiments

Starting from Day 2, both the experimental and control groups received 3-methyladenine (M833793, Macklin, Shanghai, China) treatments every 48 hours, with the experimental group receiving 3-methyladenine and the control group receiving PBS. After a 14-day period, the TG-Gel was extracted and processed as previously described. Subsequently, the samples underwent RT-PCR and Western blot to assess expression levels.

Statistical Analysis

Data for all experiments were obtained from 3 independent samples, except for stiffness analyses in Fig. 1**d** that were performed on 8 independent samples and porosity analyses in Fig. 1**e** were performed on 5 independent samples. All data were expressed as mean ± SD. Pearson's correlation was employed to elucidate the relationship between matrix stiffness and ALP levels, and the analyses were conducted using SPSS statistical software (version 26.0; IBM, NY, USA). Rest of the data analysis were performed using GraphPad Prism V8.0.1 (GraphPad Software, San Diego, CA, USA). Data in Figs. 1,2,3,4,5, one-way ANOVA with Turkey's test was used to compare differences among four groups when the data follows a normal distribution. Data in Fig. 6 was used to *t*-test to compare differences among two groups. The significance was set at $p < 0.05$.

Results

Identification of BMSCs

Using flow cytometry to identify cell surface antigens, the two negative antigens were CD34 and CD45, and the two positive antigens were CD73 and CD90. The analysis indicated that CD34- and CD45-positive cells comprised 95.5 % of the total population, while CD73-positive cells constituted only 0.022 %, and CD90-positive cells represented 0.13 %. The cultured cells possessed bone mesenchymal stem cell characteristics (Fig. 1**a**). We performed

Table 2. Primer sequences of *GAPDH* and target genes.

Target genes (rat)	Primer pairs (5′ → 3′)
RUNX2	Forward: CTGGCGGTGCAACAAGAC Reverse: AACAGCGGAGGCATTTCG
ALP	Forward: CCTTACCAACTCTTTTGTGCCAG Reverse: GCATTAGCTGATATGCGATGTCC
BMP2	Forward: TTCCATCACGAAGAAGCCGT Reverse: GAAACTCGTCACTGGGGACA
Beclin-1	Forward: GCATGGAGCAGCAACACAGTCTG Reverse: GGCACAGTGGACAGTTTGGCACAA
ATG7	Forward: AGTGCCTTGGATGTTGGGTT Reverse: GGTGGGAGCACTCATGTCAA
ATG5	Forward: GTGGAGGCAACCTGACCAGAAAC Reverse: GTGGAGGAAAGCAGAGGTGATGC
GAPDH	Forward: TCAAGAAGGTGGTGAAGCAGG Reverse: TCAAAGGTGGAGGAGTGGGT

adipogenic induction cultures of BMSCs, which underwent adipogenesis and formed ample lipid vacuoles, as demonstrated by Oil Red O staining (Fig. 1**b**).

Characterization of TG-Gel

TG-Gel's Mechanical Characteristics

The TG-Gel's mechanical characteristics were evaluated with a focus on stiffness and porosity, as illustrated in Fig. 1**d**,**e**. The TG-Gel displayed variations in stiffness corresponding to different gel concentrations. Generally, the stiffness of TG-Gel increased as the gelatin concentration rose, with 8 % TG-Gel demonstrating the highest stiffness at 215.14 kPa. This was followed by 6 % (108.67 kPa), 4 % (58.59 kPa), and 2 % TG-Gel (13.3705 kPa).

Conversely, higher gelatin concentrations led to decreased porosity in TG-Gel. Specifically, 2 % TG-Gel displayed the highest porosity at 61.54 %, followed by 4 % (56.28 %), 6 % (34.17 %), and 9 % TG-Gels (20.28 %). These findings underscore the potential for using gelatin concentration control as a direct means to tailor the TG-Gel's stiffness, enabling the assessment of how substrate stiffness affects cellular responses.

Cytotoxicity Test Results

The CCK-8 assay was employed to assess the cellular reaction to the TG-Gel (Fig. 1**f**). The findings revealed that cell viability in the 4 % TG-Gel was slightly higher compared to the 2 %, 6 %, and 8 % TG-Gels, although the differences were not statistically significant.

Effect of Matrix Stiffness on BMSCs Osteogenic Differentiation

The osteogenic differentiation of BMSCs in TG-Gel was evaluated using ALP and Alizarin red S staining, alkaline phosphatase (ALP) activity assays, and measurements of osteogenic gene and protein levels (Figs. 2,3).

ALP is one of the functional enzymes that early reflects the survival ability of osteoblasts during cell osteogenic differentiation. BMSCs in the hydrogels expressed ALP spontaneously (Fig. 2**b**). On Day 7, cells within the 8 % TG-Gel exhibited the highest ALP activity levels, succeeded by those in the 6 % TG-Gel and 4 % TG-Gel, with the lowest levels observed in the 2 % TG-Gel ($p < 0.05$) (Fig. 2**c**). Both the ALP activity assay and staining indicated that a stiff substrate promoted osteogenic differentiation, while a softer platform did not support osteogenesis. Pearson correlation analysis using SPSS revealed a significant positive correlation between matrix stiffness and ALP levels ($r = 0.853$, $p < 0.01$). This indicates a significant association between matrix stiffness and the osteogenic marker ALP within a certain stiffness range, with ALP levels increasing as matrix stiffness increases. (Fig. 1**g**).

Furthermore, after 14 days of osteogenic induction culture of BMSCs, exploring the effect of matrix stiffness on BMSCs osteogenic differentiation can be achieved by detecting the osteogenic markers mRNA and protein expression levels from different groups. The 8 % TG-Gel group showed upregulated RUNX2, ALP and BMP2 mRNA expression compared with the other groups (Fig. 2**d**), and the 8 % TG-Gel group exhibited higher RUNX2, BMP2 and osteocalcin protein expression than the 6 % TG-Gel, 4 % TG-Gel and 2 % TG-Gel groups on Day 7 (Fig. 3**b**,**c**). Additionally, RUNX2 immunofluorescence staining was performed, and higher expression was shown on rigid matrix, suggesting that the stiffness of the matrix increased the level of osteogenesis (Fig. 3**a**).

To further investigate the impact of matrix stiffness on bone formation, Alizarin Red S staining was carried out following 21 days of cell culture in TG-Gel to detect calcium deposition indicative of bone nodule formation. Fig. 2**b** illustrates the presence of calcium deposition. As the outcomes of Alizarin Red S staining, the 8 % TG-Gel ex-

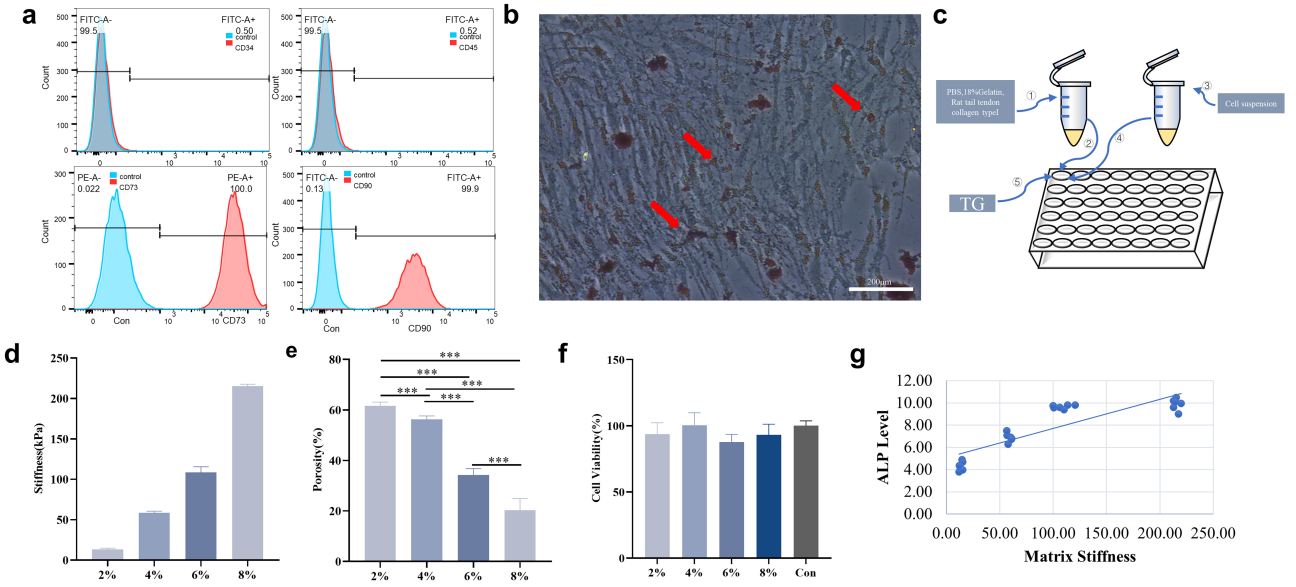

Fig. 1. Characterization of BMSCs and TG-Gel. (**a**) Flow cytometry for CD34, CD45, CD73 and CD90 expression in BMSCs. The percentage of CD34/CD45/CD73/CD90 cells among total BMSCs is indicated. (**b**) Oil Red O staining (red arrows indicate) of BMSCs with adipogenic media. Scale bar: 200 μm. (**c**) Schematic representation of the fabrication of TG-Gel of varying stiffnesses. (**d**) Stiffnesses of TG-Gel with different gelatine concentrations; eight different samples were tested as indicated. (**e**) Porosity of TG-Gel. The porosity of a TG-Gel decreases with an increase in the gelatin concentration. Data are the mean ± standard deviation, from 5 samples, significant differences (*** $p < 0.001$). (**f**) CCK-8 assays. The CCK-8 assay indicated that cell viability was not significantly different among the 4 groups. (**g**) Correlation between matrix stiffness and ALP levels (r = 0.853). All statistics were run using a one-way ANOVA with Turkey's test. The experimental control involves inter-group mutual comparison. BMSCs, bone marrow mesenchymal stem cells; TG-Gel, transglutaminase-Gelatin; CCK-8, Cell Counting Kit-8; ALP, Alkaline phosphatase.

hibited the highest calcium deposits over the course of 21 days, succeeded by the 6 % TG-Gel and the 4 % TG-Gel. Conversely, BMSCs cultivated within the 2 % TG-Gel exhibited noticeably reduced calcium deposition in comparison to those within firmer substrates. This further supports the hypothesis that the stiffness of the matrix plays a pivotal role in osteogenic differentiation.

Influence of Matrix Stiffness on Autophagy

We used TEM to demonstrate the representative ultrastructure of autophagosomes in seed cells of two groups. The results showed that more autophagosomes were observed when the BMSCs were treated with osteogenic induction medium (Fig. 2**a,b**).

To further verify the impact of stiffness on cell autophagy-related markers, we conducted qPCR analysis to examine mRNA expression levels. The results demonstrated that the mRNA expression of *Beclin-1*, *ATG5*, and *ATG7* was elevated in the 6 % TG-Gel and 8 % TG-Gel groups when compared to the 2 % TG-Gel and 4 % TG-Gel groups (Fig. 4**c**).

Likewise, the Western blot findings exhibited a consistent pattern. On the rigid matrix, there was notably greater protein expression of LC3II, Beclin-1, and ATG5 in comparison to the other groups (Fig. 5**b,c**).

MDC staining was utilized to examine BMSC autophagy across distinct groups. As depicted in Fig. 4**a**, in comparison to the soft group, the stiff groups exhibited a higher quantity of MDC-positive stained cells with intensified staining (Fig. 5**a**).

Furthermore, ATG5 immunofluorescence staining was performed, and higher expression was shown on rigid matrix.

These findings indicate that a rigid microenvironment is more conducive to BMSC autophagy compared to a softer substrate.

Expression of Osteogenic Markers after Inhibiting Autophagy

To show that substrate stiffness governs BMSC osteogenic differentiation via cell autophagy, we performed inhibitor experiments to revalidate the link betwixt osteogenic differentiation and autophagy.

Samples were subjected to 3-methyladenine treatment to reduce autophagic expression, and the mRNA expression levels of *RUNX2*, *BMP2* and *ALP* were decreased, as shown by qPCR analysis (Fig. 6**a**). Furthermore, Western blot analysis showed that the expression levels of RUNX2, BMP2 and osteocalcin proteins were decreased by 63.2 %, 66.7 % and 46.1 %, respectively (Fig. 6**b,c**). Furthermore, OCN immunofluorescence staining was performed, and lower expression was shown on inhibitor group (Fig. 6**d**).

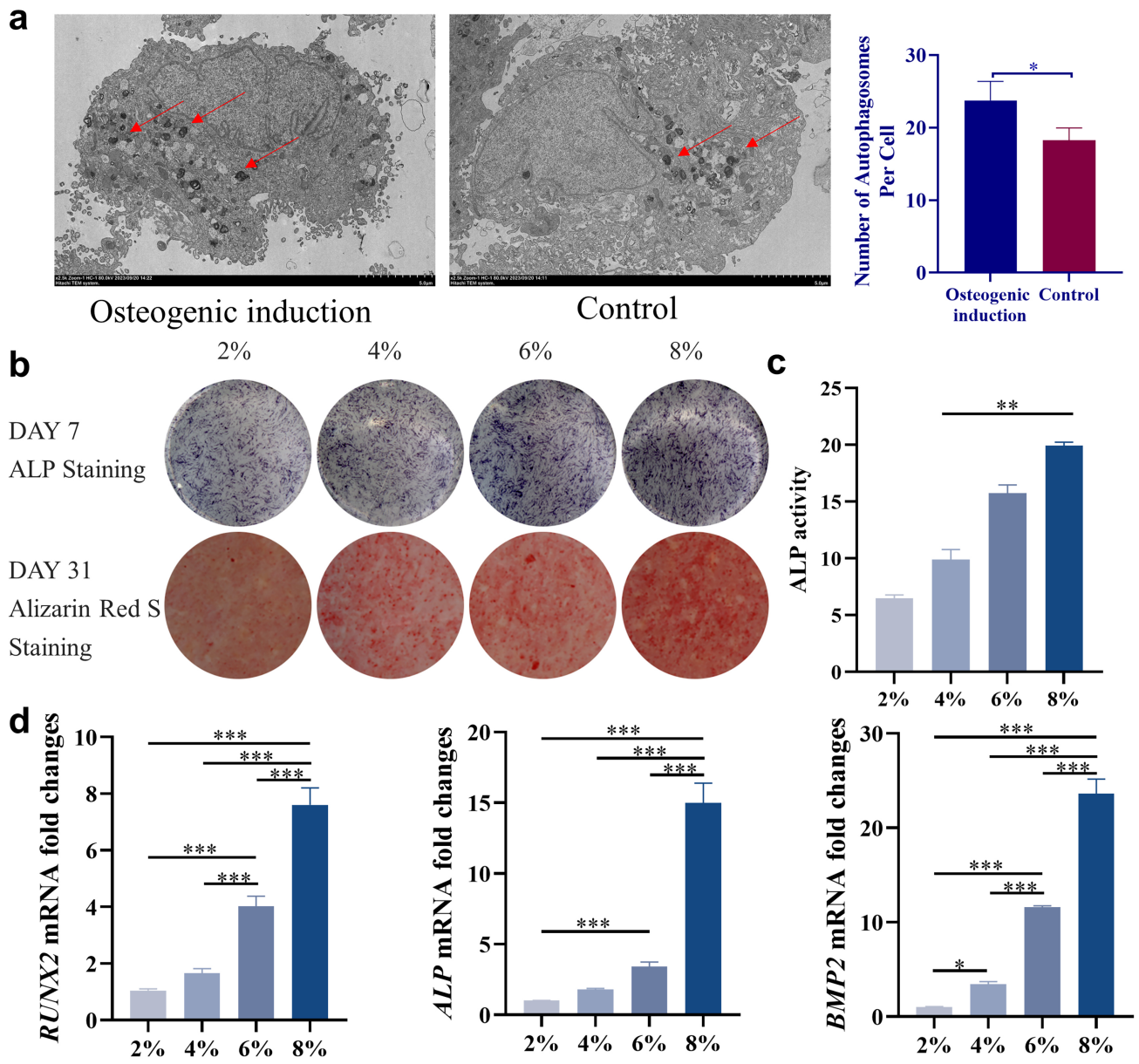

Fig. 2. Matrix rigidity induces spontaneous osteogenesis. (**a**) Electron microscopy of BMSCs. Red arrows indicate autophagomes. Scale bar: 5 µm. (**b**) ALP staining (upper) and Alizarin Red S staining (lower) of BMSCs encapsulated in 2 %, 4 %, 6 % and 9 % TG-Gels over culture periods of 7 and 14 days. (**c**) ALP activity assay. (**d**) mRNA expression of *RUNX2*, *ALP* and *BMP2* in hydrogels of different stiffnesses. Data are presented as the means ± SDs (n = 3), *$p < 0.05$, ** $p < 0.01$, *** $p < 0.001$. All statistics were run using a one-way ANOVA with Turkey's test. The experimental control involves inter-group mutual comparison.

Inhibitor experiments yielded evidence suggesting that autophagy could have a significant role in BMSC osteogenic differentiation.

Discussion

Cells exhibit responses to the mechanical properties of the extracellular matrix (ECM), such as stiffness, pore size, and dynamic vibrations. Understanding how material stiffness impacts cell fate is crucial for designing environments that guide cell behavior and tissue regeneration (Saraswathibhatla *et al*., 2023; Xue *et al*., 2019). In this study, the synthesized 3D hydrogel is composed of three components: 3D hydrogels used were composed of three parts: (1) gelatin, (2) rat tail tendon collagen type I and (3) TG, a crosslinking agent. TG-Gel, with its tunable matrix stiffness for supporting cell growth, cell adhesion, survival, and organization has been widely used in 3D cell culture research (Fang *et al*., 2014). TG acts as a crosslinking agent with gelatin, resulting in chemical crosslinking. The matrix stiffness of TG-Gel can be adjusted by modulating the gelatin concentration conveniently. Cells have been reported to tolerate the cross-linking process well, and the activity of the exogenous transglutaminase may be termi-

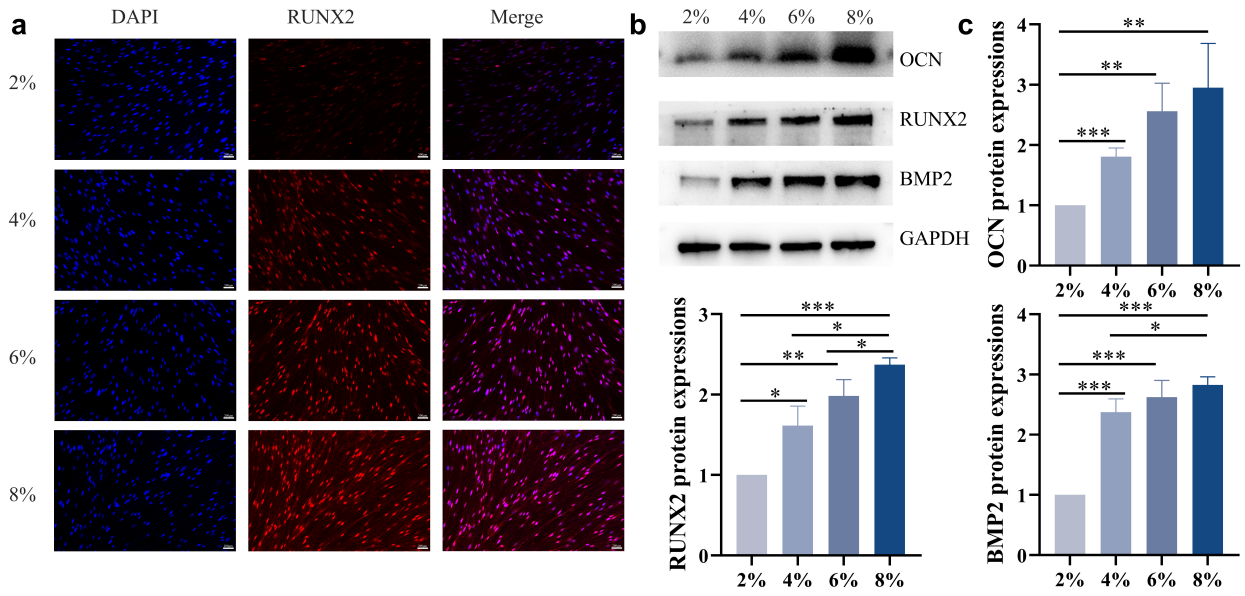

Fig. 3. Expression of osteogenesis-related proteins. (**a**) Fluorescence images of RUNX2 on the matrix of the indicated stiffness. Scale bar: 200 μm. (**b**) Western blot of OCN, RUNX2 and BMP2 protein expression in hydrogels of different stiffnesses. (**c**) Statistical analysis of the protein expression of OCN, RUNX2 and BMP2 in substrates with different stiffnesses. Scale bars are 200 μm. Data are presented as the means ± SDs (n = 3), * $p < 0.05$, ** $p < 0.01$, *** $p < 0.001$. All statistics were run using a one-way ANOVA with Turkey's test. The experimental control involves inter-group mutual comparison. OCN, osteocalcin.

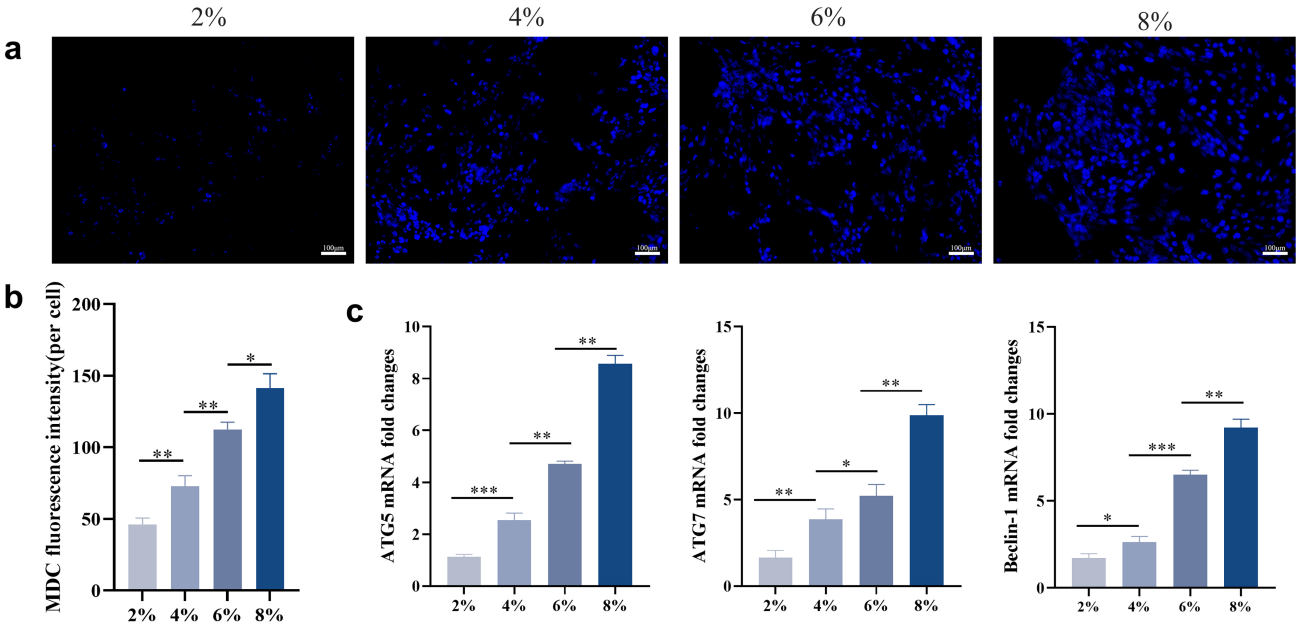

Fig. 4. Autophagy level analysis of different groups. (**a**) MDC staining for BMSCs autophagy detection. Scale bar: 100 μm. (**b**) MDC fluorescence intensity (per cell). (**c**) mRNA expressions of *ATG5*, *ATG7* and *Beclin-1* in hydrogels of different stiffness. Scale bars are 100 μm. Data are presented as means ± SD (n = 3), * $p < 0.05$, ** $p < 0.01$, *** $p < 0.001$. All statistics were run using a one-way ANOVA with Turkey's test. The experimental control involves inter-group mutual comparison. MDC, Monodansylcadaverine.

nated by cell-secreted proteinases (Chen *et al*., 2014). The current CCK-8 experiments reveal excellent cell viability and functionality throughout the gel, indicating that the decrease in the porosity of the TG-Gel did not hinder nutrient diffusion and gas exchange, as the cells exhibited proper survival and functionality throughout the entire gels. The synthesized TG-Gel employed in this research provides a pragmatic model in exploring the influence of matrix stiff-

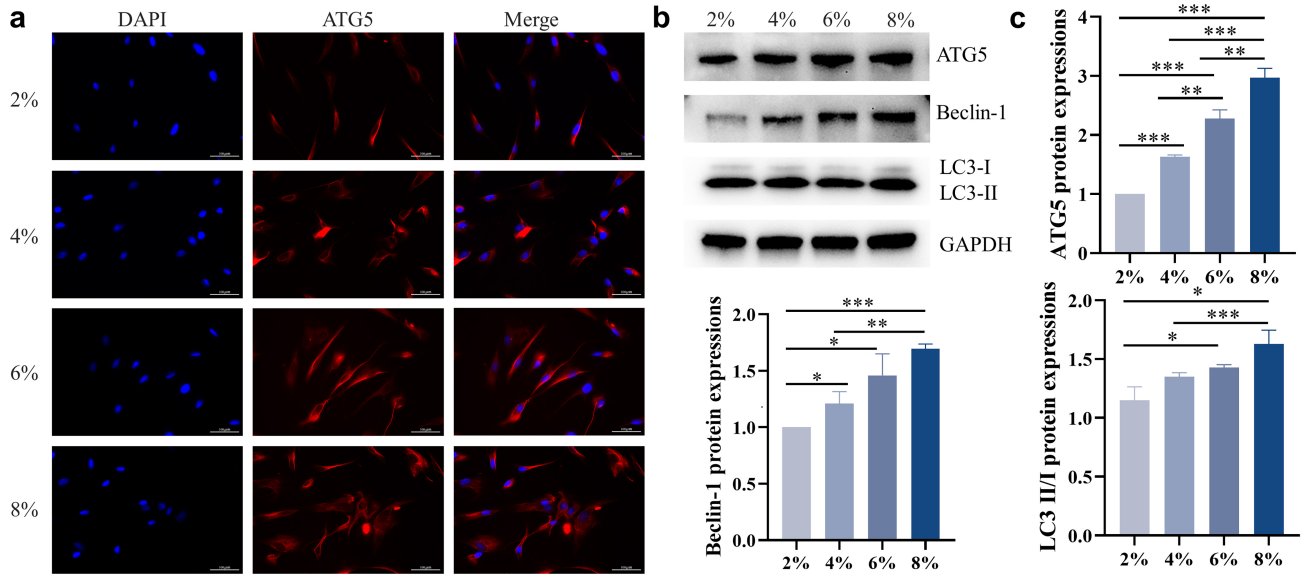

Fig. 5. Expression of autophagy-related proteins. (**a**) Fluorescence images of ATG5 on the matrix of the indicated stiffness. Scale bar: 100 µm. (**b**) Western blot of ATG5, Beclin-1 and LC3 II/LC3 I protein expression in the hydrogels of different stiffnesses. (**c**) Statistical analysis of the protein expression of ATG5, Beclin-1 and LC3 II/LC3 I in substrates of different stiffness. Scale bars are 100 µm. Data are presented as the means ± SDs (n = 3), * $p < 0.05$, ** $p < 0.01$, *** $p < 0.001$. All statistics were run using a one-way ANOVA with Turkey's test. The experimental control involves inter-group mutual comparison.

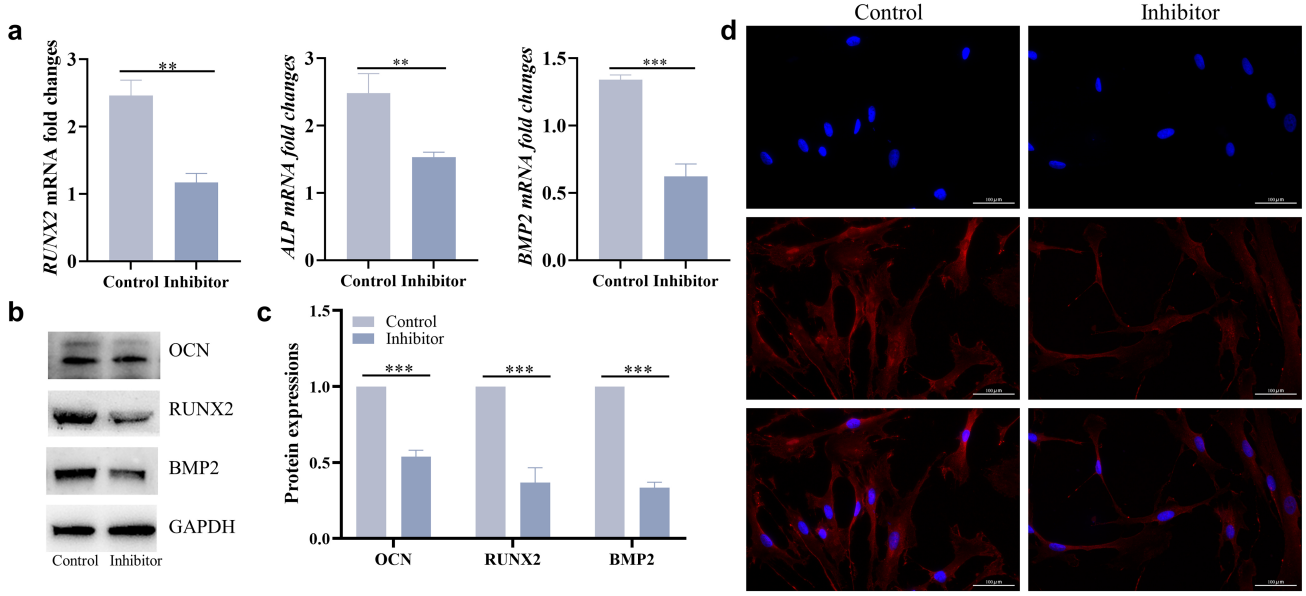

Fig. 6. Results of the inhibitor study. (**a**) mRNA expression of *RUNX2*, *ALP* and *BMP2* in hydrogels of different stiffnesses. (**b,c**) Western blot analyses of OCN, RUNX2 and BMP2 protein expression in hydrogels of different stiffnesses. (**d**) Fluorescence images of OCN on different groups. Scale bar: 100 µm. Data are presented as the means ± SDs (n = 3), ** $p < 0.01$, *** $p < 0.001$. All statistics were run using *t*-test to compare differences among two groups. The experimental control involves inter-group mutual comparison.

ness on cellular fate in osteogenic differentiation. The development of the osteoblast characteristics happens in two separate phases. In the initial phase, cells undergo proliferation while the extracellular matrix matures. Specific proteins linked to the bone cell characteristics, such as ALP, can be identified during this phase, which spans approximately 10–15 days. In the subsequent phase of osteoblast phenotype development, the matrix mineralizes, and late bone markers like osteocalcin (OCN) are persisted for up to 25–30 days (Franceschi *et al*., 2007). OCN has the capacity to bind with Ca^{2+} ions, thereby playing a role in the regulation of calcium ion balance and bone mineralization (Ducy *et al*., 1996). Throughout the process of osteogenic cell differentiation, multiple signaling pathways

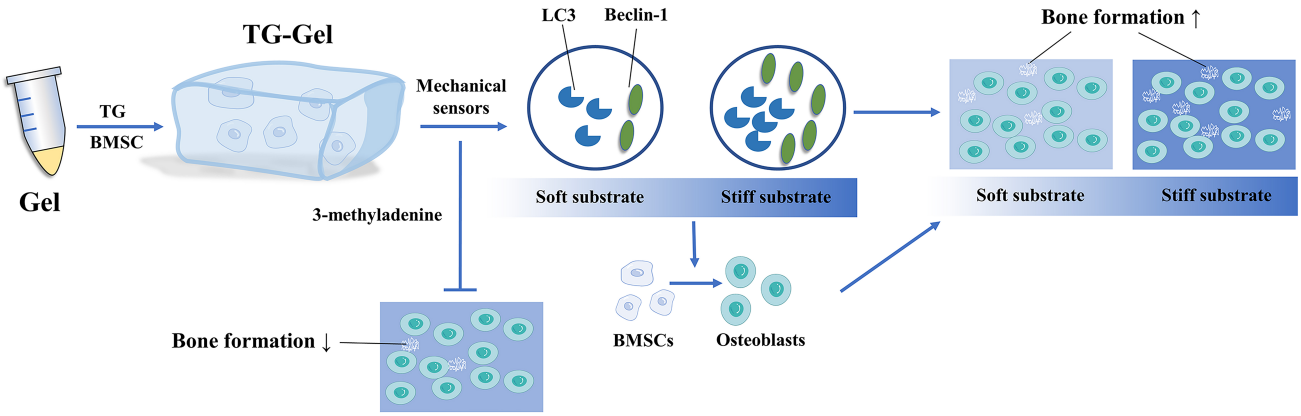

Fig. 7. Schematic diagram illustrating the relationship between matrix stiffness, autophagy and osteogenesis.

actively participate in controlling bone formation. Among these, representative molecules include BMP and RUNX2. RUNX2, a transcription factor downstream of the BMP signaling pathway, is crucial for osteogenic cell differentiation and bone formation (Franceschi *et al*., 2003). Therefore, we selected ALP, OCN, BMP, and RUNX2 as marker molecules to investigate the influence of substrate stiffness on BMSCs osteogenic differentiation. Firstly, ALP staining and quantitative analysis of BMSCs cultures after 7 days of osteogenic induction revealed that ALP activity increased with increasing substrate stiffness, with significant differences observed between 4 % TG-Gel and 8 % TG-Gel ($p < 0.01$), but no significant difference between 6 % TG-Gel and 8 % TG-Gel, possibly due to the detection is in the early stage of osteogenesis. Additionally, Pearson correlation analysis between substrate stiffness and ALP activity demonstrated a significant positive correlation, suggesting a significant role of substrate stiffness in osteogenic differentiation within the studied range of stiffness. Subsequent analysis of osteogenic-related mRNA levels and protein expression in BMSCs cultures after 14 days of osteogenic induction showed an increase with increasing substrate stiffness. Alizarin Red staining conducted on BMSCs cultures after 21 days of osteogenic induction revealed that 8 % TG-Gel exhibited the most significant calcium deposition, possibly due to its substrate stiffness being closer to that of natural bone tissue. In conclusion, substrate stiffness plays a role throughout the entire osteogenic process of BMSCs, with stiffer substrate stiffness promoting BMSCs osteogenic differentiation.

A stiffer extracellular matrix more closely resembling the *in vivo* growth environment of BMSCs enables cells to respond to microenvironmental signals and differentiate into osteogenic cells that match their surroundings. In our study, we observed rapid osteogenesis on stiffer substrates, particularly with 9 % TG-Gel. Both 9 % TG-Gel with and without BMP-2 supplementation showed the highest calcium deposition and late markers of osteogenic differentiation in our *in vitro* experiments. Conversely, ALP activity and early markers of osteogenic differentiation were more pronounced in 6 % TG-Gel (as shown in Figs. 3,5). The enhanced osteogenesis on 8 % TG-Gel may be attributed to its matrix stiffness, which closely mimics the native tissue environment (Engler *et al.*, 2006). BMSCs in this stiffer matrix can directly sense the stiffness and differentiate into the appropriate cell type. On the other hand, cells encapsulated in 6 % TG-Gel may take longer to assemble and deposit their own matrix, eventually differentiating into osteoblast-like cells at later time point, and this was consistent with the finding of Tan *et al.* (Tan *et al*., 2023). When human BMSCs cultured in different elastic-modulus of gelatin methacryloyl (GelMA), the expression of osteogenic markers was inhibited in human BMSCs (hBMSCs) cultured in the low-elastic-modulus GelMA. And *in vivo*, hBMSCs in high-elastic-modulus GelMA was more apt to form new bone (Tan *et al*., 2023). Also, the soft and porous scaffold favors chondrogenic differentiation, while osteogenic differentiation is more prominent on the initial stiff one (Wu *et al*., 2019). In summary, matrix stiffness plays vital roles in regulating cellular responses during osteogenic differentiation.

Autophagy as a way to maintain bone homeostasis, participates in BMSCs osteogenic differentiation (Shapiro *et al*., 2014). For example, reports indicate that targeted deletion a component of the complex essential for autophagosome formation in murine models, leads to severe osteopenia due to reduced bone formation (Liu *et al*., 2013). Additionally, a high-throughput small-molecule screening assay revealed that the autophagic inducer rapamycin promotes osteoblast differentiation (Darcy *et al*., 2012). In this work, transmission electron microscopy revealed that bone marrow mesenchymal stem cells (BMSCs) treated with osteogenic induction medium exhibited more autophagosomes compared to those under conventional culture conditions, indicating the involvement of autophagy in BMSCs osteogenic differentiation. However, whether matrix stiffness affects BMSCs osteogenic differentiation in an autophagy-dependent manner remains to be fully eluci-

dated. MDC staining of autophagosomes in BMSCs cultured in TG-Gel of different stiffness for 7 days showed that the group with 8 % TG-Gel exhibited the highest fluorescence intensity, demonstrating the crucial role of stiffness in inducing BMSCs autophagy. Furthermore, the ratio of LC3 II/I represents the level of autophagy, Beclin-1 is crucial for initiating autophagosome formation, and ATG5/ATG7 play specific roles in autophagosome formation originating from late endosomes and autophagosome conversion to autolysosomes, serving as core players in autophagy. Therefore, further mRNA and protein expression level analysis of autophagy-related markers in BMSCs cultured under osteogenic induction for 14 days across different groups confirmed that autophagy levels increased with the increase in matrix stiffness. By inhibiting autophagy with 3-methyladenine on the second day of BMSCs differentiation, we observed decreased mRNA levels of RUNX2, ALP, and BMP2 on the seventh day, as well as reduced protein expression of OCN, RUNX2, and BMP2 on the fourteenth day, confirming the correlation between autophagy and osteogenesis. Autophagy plays a role when stiffness affects BMSCs osteogenic differentiation (Fig. 7).

Conclusion

In summary, within a certain range, an increase in matrix stiffness promotes BMSCs osteogenic differentiation and matrix stiffness influences cell osteogenic differentiation in an autophagy-dependent manner. Matrix stiffness play a critical role in stem cell fate determination, and understanding how cells sense and respond to matrix stiffness is essential for regenerative medicine. Further studies involving animal models are necessary to validate the relevance of scaffold material stiffness in bone tissue engineering applications and to assess its therapeutic potential in treating bone defects.

List of Abbreviations

BMSCs, bone marrow mesenchymal stem cells; TG-Gel, transglutaminase-Gelatin; ECM, extracellular matrix; MSCs, mesenchymal cells; MDC, Monodansylcadaverine; CCK-8, Cell Counting Kit-8; ALP, Alkaline phosphatase; EBSS, Earle's balanced salt solution; OCN, osteocalcin; GelMA, gelatin methacryloyl; hBMSCs, human BMSCs.

Availability of Data and Materials

Data available upon justified request.

Author Contributions

HFX and CYX contributed to the design of this work. BQW contributed to the interpretation of data. BQW and YQY analyzed the data and executed experiment. BQW drafted the work. HFX and CYX revised critically for important intellectual content. All authors contributed to editorial changes in the manuscript. All authors read and approved the final manuscript. All authors agree to be accountable for all aspects of the work in ensuring that questions related to the accuracy or integrity of any part of the work are appropriately investigated and resolved.

Ethics Approval and Consent to Participate

This study adhered to ethical principles and received approval from the Experimental Animal Welfare Ethics Committee of Nanjing Medical University (IACUC-2203005) for the protocols employed.

Acknowledgments

Not applicable.

Funding

This study was supported by the National Natural Science Foundation of China (82001099); Jiangsu Provincial Key Research and Development Program (BE2022797); Undergraduate Innovation and Entrepreneurship Training Program of Nanjing Medical University (202210312157).

Conflict of Interest

The authors declare no conflict of interest.

References

Chen PY, Yang KC, Wu CC, Yu JH, Lin FH, Sun JS (2014) Fabrication of large perfusable macroporous cell-laden hydrogel scaffolds using microbial transglutaminase. Acta Biomaterialia 10: 912-920. DOI: 10.1016/j.actbio.2013.11.009.

Darcy A, Meltzer M, Miller J, Lee S, Chappell S, Ver Donck K, Montano M (2012) A novel library screen identifies immunosuppressors that promote osteoblast differentiation. Bone 50: 1294-1303. DOI: 10.1016/j.bone.2012.03.001.

DeSelm CJ, Miller BC, Zou W, Beatty WL, van Meel E, Takahata Y, Klumperman J, Tooze SA, Teitelbaum SL, Virgin HW (2011) Autophagy proteins regulate the secretory component of osteoclastic bone resorption. Developmental Cell 21: 966-974. DOI: 10.1016/j.devcel.2011.08.016.

Ducy P, Desbois C, Boyce B, Pinero G, Story B, Dunstan C, Smith E, Bonadio J, Goldstein S, Gundberg C, Bradley A, Karsenty G (1996) Increased bone formation in osteocalcin-deficient mice. Nature 382: 448-452. DOI: 10.1038/382448a0.

Engler AJ, Sen S, Sweeney HL, Discher DE (2006) Matrix elasticity directs stem cell lineage specification. Cell 126: 677-689. DOI: 10.1016/j.cell.2006.06.044.

Fang J, Yang Z, Tan S, Tayag C, Nimni ME, Urata M, Han B (2014) Injectable gel graft for bone defect repair. Regenerative Medicine 9: 41-51. DOI: 10.2217/rme.13.76.

Franceschi RT, Ge C, Xiao G, Roca H, Jiang D (2007) Transcriptional regulation of osteoblasts. Annals of the

New York Academy of Sciences 1116: 196-207. DOI: 10.1196/annals.1402.081.

Franceschi RT, Xiao G, Jiang D, Gopalakrishnan R, Yang S, Reith E (2003) Multiple signaling pathways converge on the Cbfa1/Runx2 transcription factor to regulate osteoblast differentiation. Connective Tissue Research 44 Suppl 1: 109-116.

Guan J, Fujimoto KL, Sacks MS, Wagner WR (2005) Preparation and characterization of highly porous, biodegradable polyurethane scaffolds for soft tissue applications. Biomaterials 26: 3961-3971. DOI: 10.1016/j.biomaterials.2004.10.018.

Husain A, Jeffries MA (2017) Epigenetics and Bone Remodeling. Current Osteoporosis Reports 15: 450-458. DOI: 10.1007/s11914-017-0391-y.

Levato R, Visser J, Planell JA, Engel E, Malda J, Mateos-Timoneda MA (2014) Biofabrication of tissue constructs by 3D bioprinting of cell-laden microcarriers. Biofabrication 6: 035020. DOI: 10.1088/1758-5082/6/3/035020.

Liu F, Fang F, Yuan H, Yang D, Chen Y, Williams L, Goldstein SA, Krebsbach PH, Guan JL (2013) Suppression of autophagy by FIP200 deletion leads to osteopenia in mice through the inhibition of osteoblast terminal differentiation. Journal of Bone and Mineral Research: the Official Journal of the American Society for Bone and Mineral Research 28: 2414-2430. DOI: 10.1002/jbmr.1971.

Nollet M, Santucci-Darmanin S, Breuil V, Al-Sahlanee R, Cros C, Topi M, Momier D, Samson M, Pagnotta S, Cailleteau L, Battaglia S, Farlay D, Dacquin R, Barois N, Jurdic P, Boivin G, Heymann D, Lafont F, Lu SS, Dempster DW, Carle GF, Pierrefite-Carle V (2014) Autophagy in osteoblasts is involved in mineralization and bone homeostasis. Autophagy 10: 1965-1977. DOI: 10.4161/auto.36182.

Saraswathibhatla A, Indana D, Chaudhuri O (2023) Cell-extracellular matrix mechanotransduction in 3D. Nature Reviews. Molecular Cell Biology 24: 495-516. DOI: 10.1038/s41580-023-00583-1.

Shao X, Hu Z, Zhan Y, Ma W, Quan L, Lin Y (2022) MiR-26a-tetrahedral framework nucleic acids mediated osteogenesis of adipose-derived mesenchymal stem cells. Cell Proliferation 55: e13272. DOI: 10.1111/cpr.13272.

Shapiro IM, Layfield R, Lotz M, Settembre C, Whitehouse C (2014) Boning up on autophagy: the role of autophagy in skeletal biology. Autophagy 10: 7-19. DOI: 10.4161/auto.26679.

Smith M, Wilkinson S (2017) ER homeostasis and autophagy. Essays in Biochemistry 61: 625-635. DOI: 10.1042/EBC20170092.

Steinmetz NJ, Aisenbrey EA, Westbrook KK, Qi HJ, Bryant SJ (2015) Mechanical loading regulates human MSC differentiation in a multi-layer hydrogel for osteochondral tissue engineering. Acta Biomaterialia 21: 142-153. DOI: 10.1016/j.actbio.2015.04.015.

Tan K, Yang Q, Han Y, Zhuang Z, Zhao Y, Guo K, Tan A, Zheng Y, Li W (2023) Elastic modulus of hydrogel regulates osteogenic differentiation via liquid-liquid phase separation of YAP. Journal of Biomedical Materials Research. Part a 111: 1781-1797. DOI: 10.1002/jbm.a.37590.

Wu L, Magaz A, Darbyshire A, Howkins A, Reynolds A, Boyd IW, Song H, Song JH, Loizidou M, Emberton M, Birchall M, Song W (2019) Thermoresponsive Stiffness Softening of Hierarchically Porous Nanohybrid Membranes Promotes Niches for Mesenchymal Stem Cell Differentiation. Advanced Healthcare Materials 8: e1801556. DOI: 10.1002/adhm.201801556.

Xue C, Huang Q, Zhang T, Zhao D, Ma Q, Tian T, Cai X (2019) Matrix stiffness regulates arteriovenous differentiation of endothelial progenitor cells during vasculogenesis in nude mice. Cell Proliferation 52: e12557. DOI: 10.1111/cpr.12557.

Zeng C, Guo M, Xiang Y, Song M, Xiao K, Li C (2023) Mesentery AjFGF4-AjFGFR2-ERK pathway modulates intestinal regeneration via targeting cell cycle in echinoderms. Cell Proliferation 56: e13351. DOI: 10.1111/cpr.13351.

Zhang R, Ma PX (1999) Poly(alpha-hydroxyl acids)/hydroxyapatite porous composites for bone-tissue engineering. I. Preparation and morphology. Journal of Biomedical Materials Research 44: 446-455. DOI: 10.1002/(sici)1097-4636(19990315)44:4<446::aid-jbm11>3.0.co;2-f.

Editor's note: The Scientific Editor responsible for this paper was Fergal O' Brien.